Desalination and Water Treatment
www.deswater.com

doi: 10.5004/dwt.2023.29512

292 (2023) 84–96
April

Geochemical effects of different types of mine water on the weathered coal gangue after coal seam backfill mining: an example from Shandong mining area, Northern China

Dong-jing Xu[a,*], Kai-ming Ji[a], Jin-jin Tian[a], Tian-hao Liu[b]

[a]*College of Earth Sciences and Engineering, Shandong University of Science and Technology, 579 Qianwangang Road, Qingdao City, Shandong Province, China, Tel.: +86 15066296109; email: xudongjinggg@126.com (D.-j. Xu), Tel.: +86 17635841620; email: jkm153609@163.com (K.-m. Ji), Tel.: +86 15621482891; email: tianjinjin2012@163.com (J.-j. Tian)*
[b]*Shandong Land Development Group Co., Ltd., Jinan, Shandong 250014, China, Tel.: +86 17853267169; email: ddliutianhao@163.com*

Received 11 November 2022; Accepted 29 March 2023

ABSTRACT

When using weathered gangue as the filling material for mine filling mining, karst water quality changes greatly as the underlying Ordovician limestone karst water rises to the goaf and interacts with the gangue. At present, there are few studies on the causes of changes in water quality indicators under the interaction of water-coal gangue in the goaf after coal mining. Karst water and weathered gangue batch soaking experiments in different mining areas simulated the above process. The pH change was mainly controlled by the concentration of gangue minerals, followed by cation exchange reaction. In addition, the initial pH value of Zhai-zhen No. 3 karst water on the pH change of the soaking solution cannot be ignored. Oxidation–reduction potential (ORP) changes are related to the control of different oxidants at each reaction stage. The karst water bodies of Bai-zhuang No. 1 and No. 2 Zhai-zhen are both catalyzed by Fe^{3+} and dissolved oxygen (DO), showing a similar change trend. However, Zhai-zhen No. 3 water is controlled by Fe^{3+}, DO and pH catalysts, and the ORP changes were the opposite of the first two groups. The change in total dissolved solids (TDS) is mainly related to the dissolution and adsorption rate of clay minerals. For karst water samples, the initial pH and the type and content of enriched cations affect TDS changes. The results of this study provide theoretical support for solving the problem of karst water pollution control in mining areas, and provide guidance for the utilization and environmental governance of coal gangue in mining areas.

Keywords: Ordovician limestone karst water; Weathered coal gangue; Water pollution; Filling mining

1. Introduction

Coal gangue is harmful solid waste generated during coal production and processing and after the closure of coal mines. According to statistics [1], there are more than 1,500 coal gangue hills in China, which accumulated exceeded 3.5 billion tonnes of coal gangue, account for about 40% of China's industrial solid waste production. In mining areas, a considerable amount of coal gangue is naturally and loosely piled up around the mine, which is cone-shaped or valley-shaped. Dust formed by weathering and erosion of coal gangue and CO and SO_2 emitted by residual coal spontaneous combustion will deteriorate the atmospheric quality of the mining area. The acidic wastewater produced through the precipitation and dissolution of coal gangue mountains pollutes the surrounding soil and water bodies, and the stacking of coal gangue also occupies considerable land and causes a waste of resources. Currently, coal gangue is mainly used to generate electricity, prepare building materials, pave a roadbed, synthesise chemical products, produce fertilisers, and

* Corresponding author.

fill mines [2]. Filling mining as a new coal mining method is the coal gangue filling into the mine mining area to assist the coal mining technology. The method has attracted considerable attention and is widely used for safe coal mining. Filling mining technology can not only mitigate the influence of coal gangue stacking on the atmosphere, soil, and surface water but also address the problems of surface subsidence and collapse caused by coal mining. Furthermore, coal resources can be mined in protected areas and villages [3,4]. This mining technology has considerable environmental, economic, and social implications [5,6]. In the mining areas in northern China, the mining of most coal-bearing strata is threatened by Ordovician limestone aquifers. As the main water supply source for mining residents, Ordovician limestone karst is situated deep underground and exhibits excellent water quality, but it is highly environment sensitive and can be easily polluted. As displayed in Fig. 1, when Ordovician limestone karst water enters goaf, pollutants are gradually released into the surrounding environment. The migration of toxic and harmful components in solid waste in the goaf to the water causes water pollution, which harms the surrounding environment and human health. For the solid waste in the goaf, the reaction temperature, pressure, pH, and redox conditions are all related to the goaf environment. The experimental conditions selected by previous studies often use room temperature as the experimental temperature or use distilled water to soak and dissolve, under-considering the environment of the goaf area. Studies on the interaction between water (karst water) and rock (coal gangue) have focused on the geochemical characteristics of heavy metal elements in coal gangue [7–10], coal gangue pollution due to the groundwater environment [11–13], the migration mechanism of heavy metal elements [14–16], and the improvement of filling technology [17]. However, there are few studies on the water quality index changes and related causes of karst water affected by coal gangue under the condition filling mining used mining of weathered coal gangue.

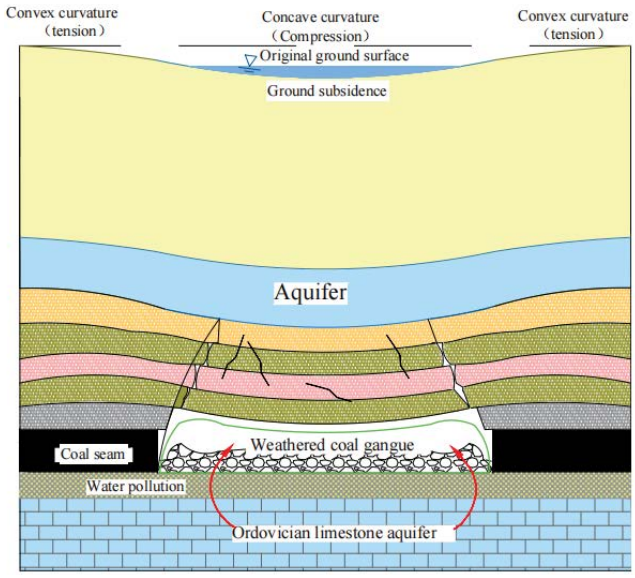

Fig. 1. Schematic of Ordovician limestone water pollution from the weathered coal gangue left in goafs or backfills.

To study the influence of weathered coal gangue on the karst water quality indexes under filling mining, the site Ordovician limestone karst water in the mining area was used as the soaking solution together with coal gangue for experiments, meanwhile, the actual temperature and closed environment of the goaf was simulated. The basic water quality parameters pH, (oxidation–reduction potential [ORP], total dissolved solids [TDS], dissolved oxygen [DO], and electrical conductivity [EC]), anions and cations (sodium, calcium, sulfate, chloride, etc.) before and after soaking in this study were analysed and discussed. The variation and the original mode of three key water quality indexes including the pH, ORP, and TDS before and after soaking in coal gangue under various karst water conditions were mainly considered, which can be used as theoretical guidance for investigating the interaction mechanism between water (karst water) and rocks (coal gangue) after coal mining, and provided critical theoretical support for comprehensive utilisation of coal gangue and water environment treatment in mining areas in the future.

2. Materials and methods

2.1. Overview of the study area

The study area involves three mining areas (Fig. 2): Hong-qi coal mine, Bai-zhuang coal mine, and Zhai-zhen mine field. Hong-qi coal mine is located in the northeast of the Ju-ye coalfield. The coal-bearing strata are North China Carboniferous ~Permian of sea–land interaction deposition, the base of coal system is Ordovician limestone, and the overburden of coal system is Quaternary loose sediments and Paleogene red sandstone and mudstone [18]. Bai-zhuang coal mine is in the middle and west of the Fei-cheng coalfield, with stable strata deposition, and its thickness, lithology, and contact relationship of strata are consistent with the strata zoning in western Shandong. The Ordovician limestone layer is widely exposed on the surface of the earth; therefore, it is directly affected by atmospheric precipitation. The water content is extremely high, the salinity is 247–681 mg/L, belongs to low mineralization water, and the water quality type is HCO_3-Ca·Mg, water quality belongs to class I-III according to GB/T 14848-2017 Groundwater Quality Standard [19]. Zhai-zhen coal mine is located in Zhai-zhen, Xin-tai city. In the shallow of this region, it belongs to the moderately rich aquifer, and its supply route is mainly affected by a small amount of outcrop atmospheric precipitation in the north wing. The Ordovician limestone water mainly is high-pressure karst fissure still water. Its mineralization degree is 544 to 1,252 mg/L, belongs to medium mineral degree water, water quality type is SO_4-K Ca Na Mg, and water quality belongs to class II-IV according to GB/T 14848-2017 [20].

2.2. Sample preparation and testing

In this study, coal gangue weathered for a year in Hong-qi coal mine was used as the experimental solid sample. Coal gangue was piled outside the mine in the open air, and the snake-shaped distribution method and polypropylene shovel were used to collect coal gangue at 15 points. Equal amounts of coal gangue were obtained from each point. The samples

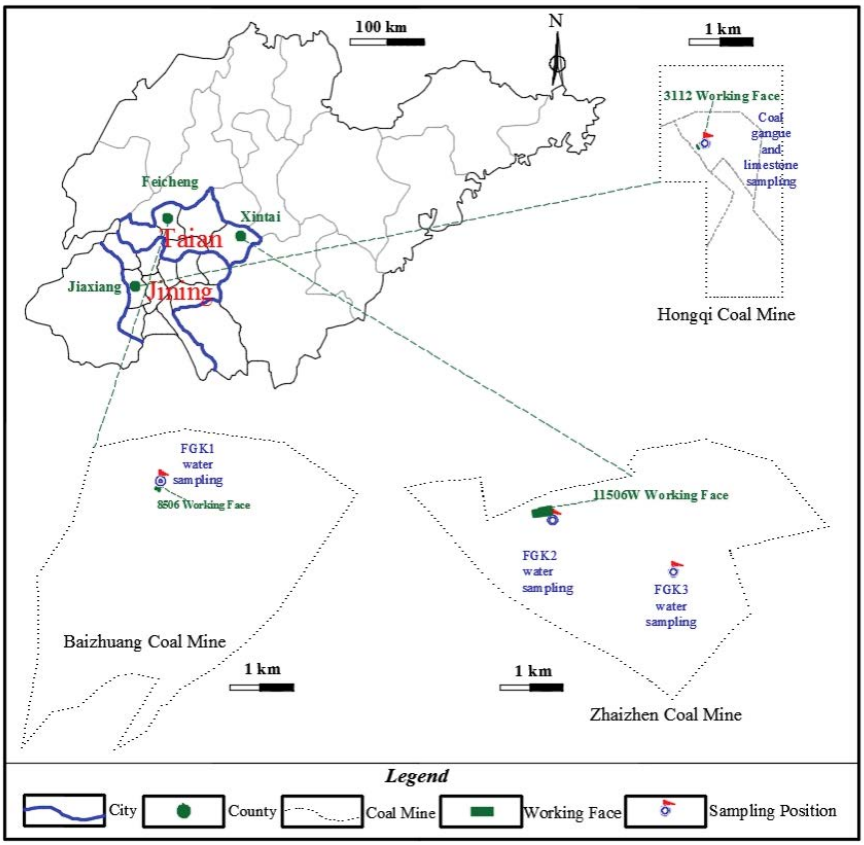

Fig. 2. Location of the coal mines.

were completely mixed as the experimental weathered coal gangue sample. The collected weathered coal gangue was crushed using a jaw crusher, and coal gangue particles with diameters between 0.45 and 3.2 mm were selected. Next, 2,000 g of weathered coal gangue samples were weighed and wrapped in foil paper and placed in a drying dish for subsequent use.

The Ordovician limestone water from Bai-zhuang and Zhai-zhen coal mines was used as soaking water. Sampling point 1: Ordovician limestone karst water of Bai-zhuang coal mine with the water level of −250 m and water pressure of 1.9 MPa, respectively; Sampling point 2: Ordovician limestone karst water of Zhai-zhen coal mine a water level of −549.8 m and water pressure of 2.8 MPa in the hole; Sampling point 3: Ordovician limestone karst water of Zhai-zhen coal mine the water level is −395.07 m, and the water pressure in the hole is 2.05 MPa. In order to maintain the similarity of the simulation test as much as possible, the groundwater is sealed at a constant temperature, and then the sealed bottle and incubator are used to simulate the actual mining area environment in the subsequent soaking test.

Mineral composition analysis using the ARL Perform X4200 X-ray fluorescence spectrometer (measurement method: wavelength dispersion sequence scanning type; analysis element range: O-U3; content range: ppm to 100%). The main chemical components were analyzed by a D/max-2500v/pc X-ray diffractometer (Cu target, Kα radiation, step size 0.02°, power 40 kV, 40 mA, the scan speed is 10°/mm and scan range is 5°~80°) produced by Rigaku Corporation of Japan.

2.3. Soaking experiment

According to the drilling experiment results of Wang Xiao-chen and Shi Long-qing in Jia-xiang coal mine area and rock water storage coefficient, the relationship between coal gangue and mine water in the goaf can be obtained [21], and 10 g of coal gangue samples were taken and placed in a plug cone bottle containing 100 mL immersion liquid to make the water-rock mass ratio 10:1. The four soaking solutions, which were marked as WGK1, WGK2, WGK3, and WGK4, used in the experiment were the Ordovician limestone water samples obtained from Bai-zhuang, two boreholes in Zhai-zhen and ultrapure water. The blank control test was WGK4, the conical bottles mixed with water were resting in a 40°C incubator, and samples were removed at seven sampling times 1, 2, 4, 7, 15, 25, and 35 d after immersion, three samples of each type samples were removed for parallel testing. The supernatant was filtered into polyethylene bottles by using a microporous membrane with a pore size of 0.45 μm, sealed, and stored at 4°C until experimental analyses.

The pH, ORP, EC, TDS, and DO values before and after immersion were measured by a Hydrolab multi-parameter water quality analyzer. Using the Agilent 7500 inductively coupled plasma mass spectrometer (It has a rapid and simultaneously detection capability for practically all entries on

the cycle table; low detection limit (as low as ppb level); wide linear dynamic range that can directly detect concentrations between ppb to hundreds of ppm; the spectral line is simple, small interference; good accuracy and precision require a very low sample size (uL to mL); fast analysis speed (1~3 min per sample)) and the ICS-600 ion chromatograph of the Thermo-Fisher Company in the American (curve range 0–200 ug/L; speed measurement:1.00 mL/min; pressure: 1,965 psi) to measure the content of main cations (potassium, sodium, calcium, magnesium, etc.) and the anions (chloride, sulfate, nitrate, etc.), respectively.

3. Results and discussion

According to the experimental results and the correlation between water quality indexes, the basic characteristics of weathered coal gangue and karst water samples were first analysed, and the changing trend and mechanism of three key characteristic water quality indexes, pH, ORP, and TDS were analysed.

3.1. Test results of coal gangue and karst water

3.1.1. X-ray fluorescence spectrometer and X-ray diffractometer analysis of coal gangue

According to X-ray diffraction (XRD) analyses seen in Fig. 3, the main minerals of coal gangue are kaolinite and quartz, and its secondary minerals are calcite, pyrite, sanidine, ankerite, smectite, illite, and muscovite, this result is consistent with the analysis report of Ju-ye coal exploration [22]. However, due to the influence of mineral analysis software, although XRD shows the presence of minerals, minerals with less than 3% content are not demonstrated.

It can be seen from the table of oxide content in coal gangue (Table 1) that the samples mainly constitute SiO_2 (49.77%) and Al_2O_3 (36.38%), and the concentrations of SiO_2, Al_2O_3, and Fe_2O_3 in the samples account for 89% of the total oxides. The ratio of SiO_2/Al_2O_3 in the coal gangue samples is larger than the theoretical ratio in kaolinite (1.18) [23], which indicated that the tested coal gangue samples mainly constitute kaolinite minerals and quartz, which is consistent with the XRD results.

3.1.2. Potential contamination assessment of water quality parameters of the initial water sample

According to the test results, the summary of initial indicators of water samples is presented in Table 2. According to Table 2, the quality of karst water in Bai-zhuang satisfies water quality parameters of Class III standard value of groundwater environmental quality (GB/T 14848-93) [24]. The water quality of Zhai-zhen is poor, and its ion concentration considerably exceeds the standard. The TDS, Fe^{3+}, Na^+, and SO_4^{2-} of karst water in No. 2 Zhai-zhen exceeded the Class III of groundwater environmental quality standard (GB/T 14848-93), and the pH, Na^+, and SO_4^{2-} of No. 3 Zhai-zhen karst water exceeded the specified value of Class III for the groundwater environmental quality standard (GB/T 14848-93). Na^+ and SO_4^{2-} exceeded the standard in the two groups of Zhai-zhen karst water, and the No. 2 water sample reached more than five times the water quality standard, which the analysis results remind we ought to focus the influence of these parameters on water quality change.

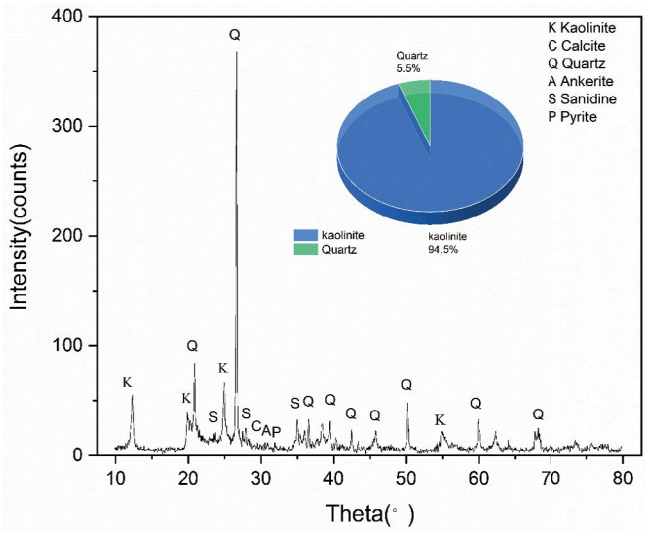

Fig. 3. Mineral X-ray diffraction analysis results plot.

Table 1
Chemical composition of weathered coal gangue

Chemical composition (%)	SiO_2	Al_2O_3	K_2O	MgO	Fe_2O_3	TiO_2	CaO	Na_2O	SO_3	ZrO_2	SrO	MnO
Percentage	49.765	36.382	3.256	3.034	2.738	2.229	0.971	0.815	0.722	0.038	0.032	0.018

Table 2
Initial indicators of karst water

Sample number	pH	Total dissolved solids (mg/L)	Total hardness (Ca^{2+}) (mg/L)	Na^+ (mg/L)	K^+ (mg/L)	Fe^{3+} (mg/L)	Cl^- (mg/L)	SO_4^{2-} (mg/L)
GB/T 14848-93	6.5~8.5	1,000	450	1,000	–	0.3	250	250
WGK1	7.64	480.3	137.80	50.8	1.3	0.32	68.33	114.39
WGK2	7.69	1,251.7	217.50	1,000	16.4	0.71	82.63	1,224.58
WGK3	9.57	543.7	29.21	1,000	11.8	0.09	6.92	368.97

3.2. pH change trend and mechanism under different immersion solutions

The data of the immersion test were reported as the average of the three parallel trials, with a pH maximum relative deviation of 10%. The pH value of gangue immersion fluid under different types of karst water is shown in Fig. 4.

Fig. 4 reveals that the pH value of WGK4 water samples in the blank control group can be categorised into three stages: rapid increase within 0–7 d, rapid decrease within 7–15 d, and slow fluctuation within 15–35 d. In the first stage, the pH value of the WGK4 water sample gradually increased with the soaking time, and reached the maximum value of 9.47 on day 7, which revealed strong alkalinity. The possible reasons were analysed: (1) the total acid production from sulphide (pyrite) oxidation on the surface of coal gangue at the initial stage of soaking was less than the total alkali production from clay minerals such as calcite [25,26]; (2) NH_4^+ produced through the dissolution of nitrogen-containing substances in coal gangue buffered the solution, and inhibited or neutralised acidic mine wastewater produced by pyrite oxidation [27,28]. In the second stage, the alkali production rate of calcite decreased, and the rapid acid production of sulphide progressed. However, silicate also entered the rapid alkali production period, and the total alkali production rate was higher than the acid production rate. The pH of the solution gradually decreased but remained alkaline. In the third stage, pyrite wrapped in coal gangue participated in the oxidation and acid-producing reactions, which continuously produced H^+, but the hydrolysis reaction of the organic acid radical and S^{2-} ionic compound consumed a certain amount of H^+ [29]. Therefore, the pH fluctuated slowly with the reaction. With the decrease in the DO concentration, the reaction did not go on endlessly. According to X-ray fluorescence (XRF) analysis results, the silicate concentration in coal gangue was higher than the sulphide concentration, that is, the total alkali-production capacity was higher than the acid-production capacity, and the pH value of the soaking solution was weakly alkaline when it reached the acid-base equilibrium [30,31].

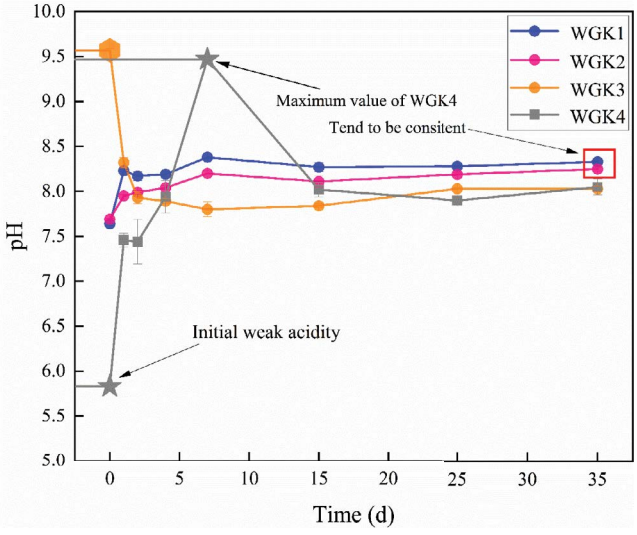

Fig. 4. Coal gangue immersion solution pH under various karst water conditions.

The changes in the pH values of WGK2 and WGK1 soaking solutions revealed the same change tendency, which can be categorised into two stages: slow increase during 0–7 d and slow fluctuation during 7–35 d. In the first stage, the pH value of WGK1 and WGK2 water samples gradually increased and reached the maximum value on day 7. The reasons were as follows: (1) karst water contains numerous ions, and the cation exchange reaction started at the initial stage of soaking with $R^{n-}X^{n+} + nH^+ = R^{n-}H^{n+} + X^{n+}$ X = K/Ca/Na/Mg; (2) at the initial stage of soaking, oxides (such as calcite) in coal gangue underwent the hydrolysis reaction, and H^+ produced by sulphide was continuously consumed, but the total alkali production rate was higher than the acid production rate. Therefore, the pH increased. In the second stage, the pyrite wrapped in coal gangue participated in the oxidation and acid production reactions to continuously produce H^+, but the hydrolysis reaction of the organic acid radical and ionic compound (such as S^{2-}) led to the consumption of a certain amount of H^+. Therefore, the pH fluctuated with the reaction. However, the initial Fe^{3+} content of the WGK2 is higher, which consumes more H^+ and has a lower pH value. With the gradual decrease in the DO concentration, the reaction did not go on endlessly. According to the XRF analysis, the silicate concentration in coal gangue was higher than the sulphide concentration, that is, the total alkali-production capacity was higher than the acid-production capacity, and the pH value of the soaking solution was weakly alkaline when it reached the acid-base equilibrium.

The change in the pH value of the WGK3 soaking solution is categorised into three stages: a rapid decrease in 0–2 d, a slow decrease in 2–7 d, and a slow rise in 7–35 d. At the beginning of immersion, with the increase in the soaking time, the pH value gradually decreased and reached the minimum value on day 7. The reasons were as follows: (1) the WGK3 water sample exhibited strong alkalinity initially, which inhibited the dissolution and release of alkaline components in clay minerals, and the oxidation of pyrite and nitrogen-containing organic compounds to produce acid increased [32]; (2) karst water contained considerable ions, and the cation exchange reaction began at the initial stage of soaking, with $R^{n-}X^{n+} + nH^+ = R^{n-}H^{n+} + X^{n+}$ X = K/Ca/Na/Mg, which consumed a part of H^+. However, at this time, the total acid production was higher than the total alkali production, and the pH decreased. After 7 d, the inhibition of the alkali-producing reaction of clay minerals gradually weakened with the decrease in the pH value, and the acid production rate gradually decreased with the consumption of sulphide. The acid-producing reaction of wrapped pyrite progressed. The total alkali production rate was higher than the acid production rate, and the pH exhibited an upward trend. With the gradual decrease in the DO concentration, the reaction did not go on endlessly. According to the XRF analysis, the silicate concentration in coal gangue was higher than the sulphide concentration, that is, the total alkali-production capacity was higher than the acid-production capacity, and the pH value of the soaking solution was weakly alkaline when it reached the acid–base equilibrium.

The pH change of the WGK4 water sample was influenced by the concentration of alkaline/acidic minerals in

coal gangue. When the acid yield of alkaline minerals was higher than that of acidic minerals, the pH increased, and vice versa, which revealed a trend of the increase first, followed by a decrease, and subsequent stabilisation. The water samples of the WGK1 and WGK2 contained numerous ions, and the cation exchange reaction started at the initial stage of soaking. Therefore, the pH change was affected by the ratio of alkaline/acidic minerals content in coal gangue and the cation exchange reaction, which revealed a trend of increase first and subsequent stabilisation. The strong initial alkaline of WGK3 water samples inhibited the dissolution of alkaline components in coal gangue, the pH change was affected by three factors, namely the content of alkaline/acidic minerals in coal gangue, cation exchange reaction, and the pH value of karst water, which revealed a trend of the initial decrease and subsequent stabilisation. According to XRF analysis of the samples, the silicate concentration in coal gangue was higher than the sulphide concentration, that is, the total alkali-production capacity was higher than the acid-production capacity, and each soaking solution was finally weakly alkaline, which revealed that the mineral concentration of coal gangue considerably influenced pH change and was the main controlling factor.

3.3. Change trend and influence mechanism of ORP value under different immersion solutions

The redox potential reflects the electrochemical properties in the immersion liquid system, which is mainly affected by the change in Fe^{2+}/Fe^{3+} forms in the immersion liquid [33]. The main chemical reactions of pyrite oxidation to produce acid were as follows:

$$2FeS_2 + 7O_2 + 2H_2O \rightarrow 2Fe^{2+} + 4H^+ + 4SO_4^{2-} \quad (1)$$

$$4Fe^{2+} + O_2 + 4H^+ \rightarrow 4Fe^{3+} + 2H_2O \quad (2)$$

$$FeS_2 + 14Fe^{3+} + 8H_2O \rightarrow 15Fe^{2+} + 2SO_4^{2-} + 16H^+ \quad (3)$$

Eqs. (1) and (3) reveal that pyrite produced a large quantity of H^+ after being oxidised by O_2 and Fe^{3+}, and O_2, H^+, and Fe^{3+} in the environment directly or indirectly affected the surface oxidation rate. Compared to the mentioned three reactions, the reaction rate represented by Eq. (2) was slow. Studies [29,34] have revealed that the oxidation of Fe^{2+} to Fe^{3+} [Eq. (2)] is the decisive step in the pyrite oxidation process. Tu [35] studied the influencing factors of this controlling step and revealed that the oxidation rate of Fe^{2+} was not only affected by the O_2 concentration but also negatively correlated with the H^+ concentration in the system. Druschel [36] revealed that when Fe^{3+} and O_2 existed simultaneously in the reaction system, the oxidation rate of these two substances was at least one order of magnitude faster than that of O_2 alone. Data from the immersion test were reported as the mean of the three parallel trials, with the maximum relative deviation of ORP and DO of 6% and 3%, respectively. The variation law of ORP and DO of the coal gangue soaking solution with time under various karst water types is displayed in Fig. 5.

Fig. 5a reveals that with the progress of time, the ORP value of the WGK4 water sample in the blank control group can be categorised into three stages: continuous decline in 0–7 d, continuous rise within 7–25 d, and stable within 25–35 d. In the first stage, the DO initial concentration in WGK4 was high, with no Fe^{3+} ion interference, and the oxidation of pyrite was mainly influenced by the DO concentration. The reaction rate of equation 1 was fast, the Fe^{2+} in the soaking solution increased, and the ORP in the solution decreased. In the second stage, according to Moses, Fe^{2+} is adsorbed on the surface of pyrite in preference to Fe^{3+} in the reaction process [37]. Eq. (2) reveals the main reaction, with the increase in Fe^{3+} in the soaking solution and the ORP value of the solution being higher. In the third stage, according to Druschel [36], when Fe^{3+} and O_2 exist simultaneously in the reaction system, the oxidation rate of pyrite was fast. At this stage, the oxidation of pyrite reached equilibrium and ORP was stable.

The ORP values of WGK2 and WGK1 water samples exhibited identical change results: the values decreased continuously during 0–4 d, increased and decreased during 4–25 d, and remained stable during 25–35 d. The reasons for the change are as follows: in the first stage, the initial Fe^{3+} concentration of the two groups of the water samples was higher, and the pyrite oxidation was mainly influenced by the Fe^{3+} concentration at the initial stage of soaking. At this time, Eq. (3) was the main reaction [38]. Fe^{2+} increased, Fe^{3+} decreased

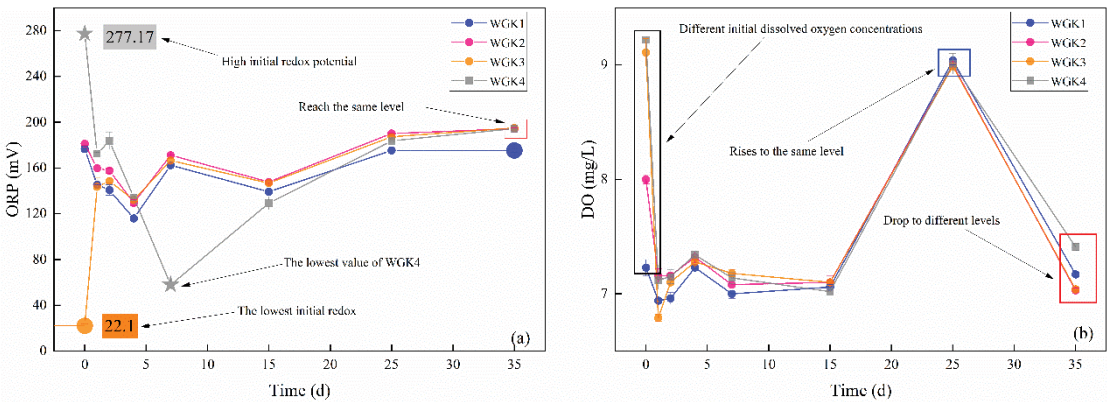

Fig. 5. Trend diagram of oxidation–reduction potential and dissolved oxygen under different karst water conditions.

in the soaking solution and the ORP value of the solution decreased. In the second stage, as Fe^{3+} consumption Eq. (3) was no longer the main process of pyrite oxidation and acid production, both Fe^{3+} and O_2 affected pyrite oxidation and acid production, and Fe^{2+}/Fe^{3+} forms were transformed and ORP fluctuated accordingly. In the third stage, according to Druschel [36], when Fe^{3+} and O_2 existed simultaneously in the reaction system, the oxidation rate of pyrite was fast; at this time, the oxidation of pyrite reached equilibrium and ORP was in a stable stage. However, after stabilization, the pH of WGK1 is higher and the content of OH^- is higher, which leads to the ORP value being lower than that of WGK2.

The ORP value of WGK3 water samples can be categorised into three stages: continuous rise between 0–2 d, fluctuations between 2–25 d, and stable stage between 25–35 d. In the first stage, WGK3 exhibited high DO initial concentration and strong alkalinity the before soaking, the reaction rate of Eq. (2) was fast, the amount of Fe^{3+} in the soaking solution increased, and the ORP of the solution increased. In the second stage, with the decrease in pH, Eq. (2) was not the main process of pyrite oxidation and acid production. Both Fe^{3+} and O_2 affected pyrite oxidation and acid production; Fe^{2+}/Fe^{3+} forms were transformed, and ORP values fluctuated. In the third stage, according to Druschel [36], when Fe^{3+} and O_2 existed simultaneously in the reaction system, the oxidation rate of pyrite was fast. At this time, the oxidation of pyrite reached equilibrium and ORP was in a stable stage.

According to the trend of change in ORP of each soaking solution and the analysis of pyrite oxidation and acid production: the change in the ORP value of the WGK4 water sample was mainly affected by the DO concentration, but the reaction emphasis differed in the initial and middle stages of the reaction, and the ORP exhibited a trend of initial decrease, followed by an increase, and subsequent stabilisation. Because the initial content of Fe^{3+} was high in the WGK1 and WGK2 water samples, the ORP changes in the early stage were controlled by Fe^{3+}. With the simultaneous action of Fe^{3+} and O_2, the ORP emerge fluctuates changes, and overall ORP showed a trend was first of all decrease, followed by fluctuation, and subsequent stabilisation. The WGK3 water sample had a low initial Fe^{3+} concentration and a high DO content and pH, which were mainly affected by DO and pH in the early stage. With the reaction, Fe^{3+} and O_2 corporate played a role, and the overall trend was an initial increase, followed by fluctuation, and subsequent stabilisation.

3.4. Analysis of the change of TDS and key influencing parameters under different immersion solutions

TDS is a comprehensive reflection of the concentration of ions in water. With water-rock interactions progress in coal mine goaf, such as the dissolution of rocks, TDS usually fluctuates. Analysis of TDS changes reveals the main reaction of underground reservoirs in coal mines and sources of main ions in water.

In the water-rock interaction, the causes of the ion concentration changes are as follows: the dissolution of sulfate minerals and silicate minerals, water–rock ion exchange, adsorption of clay minerals, precipitation of secondary minerals, and other reactions. The reaction of coal gangue immersion was analysed, which revealed that sulphide in coal gangue was less resistant to weathering than silicate minerals were, sulphide decomposed easily when exposed to sunlight and rain, and sulfate minerals (such as mirabilite, pyrite, and gypsum) dissolved preferentially compared with silicate minerals during soaking. According to XRD and XRF analyses, the main mineral components of weathered coal gangue are kaolinite and quartz. These components exhibit various adsorption forms for metal cations: ion exchange adsorption, chemical adsorption, and physical adsorption. Zhang et al. [39] revealed that the adsorption capacity of kaolinite for four ions is $Ca^{2+} > Mg^{2+} > K^+ > Na^+$. Ions exchange reaction occurred in the adsorption of clay minerals, and the metal cations on the surface of kaolinite particles exchanged with the metal cations in the solution. Studies [40] have revealed that $Ca(OH)_2$ and $Mg(OH)_2$ precipitates form easily on the surface of clay minerals, and $Ca(OH)_2$ precipitates $CaCO_3$ easily under the action of free CO_2 in the solution [41]. Wu Hong-hai and other studies have revealed that both ion exchange and adsorption modes exist when the pH value of the solution is 6.5–8, and the surface precipitation is dominant when the pH is greater than 8. However, this experiment was performed in a confined space, and the sedimentation will gradually weaken with the decrease in CO_2. Silicate minerals exhibit high solubility under acidic conditions and weak solubility under alkaline conditions. Therefore, in this experiment, silicate minerals only dissolved in the initial stage of WGK4 soaking and were slightly soluble or insoluble in the karst water samples.

3.4.1. Analysis of water quality parameter correlation and key parameters variation in the blank control group (WGK4)

SPSS19.0 was used for the factor analysis on hydro-chemical parameters, and the correlation coefficient matrix of hydro-chemical parameters of WGK4 water samples in the blank control group was as follows in Fig. 6:

In general, we argue that 0.8–1 is an extremely strong correlation, 0.6–0.8 strong correlation, 0.4–0.6 moderate correlation, 0.2–0.4 weak correlation, and 0–0.2 extremely weak correlation. Fig. 6 reveals that a strong correlation exists between TDS and SO_4^{2-} (R = 0.957), which indicates that the concentration and spatial distribution of SO_4^{2-} play a key role to TDS. The relations of TDS, sulfate, and calcium ions were 0.68,0.794, respectively, with strong correlation, which indicates that the dissolution of gypsum ($CaSO_4{\cdot}2H_2O$) has a high contribution to the TDS change of the water samples. The relations of TDS, sulfate, and sodium ions were 0.566 and 0.65, respectively, with moderate correlation, which indicates that the dissolution of mirabilite ($Na_2SO_4{\cdot}10H_2O$) also certain degree contributes to the TDS change of the water samples. A strong correlation exists between TDS and Cl^- (R = 0.794), which indicates that Cl^- concentration considerably influences TDS. Meanwhile, the relations of TDS, chloride, and sodium ions were 0.566 and 0.681, respectively, with moderate correlation, which indicates that the dissolution of rock salt (NaCl) also contributes to the TDS change of the water samples. The data from the WGK4 immersion test are reported as the average of three parallel trials, with a maximum relative deviation of 1% (TDS) and 13% (general water chemical parameters). The variation of the main

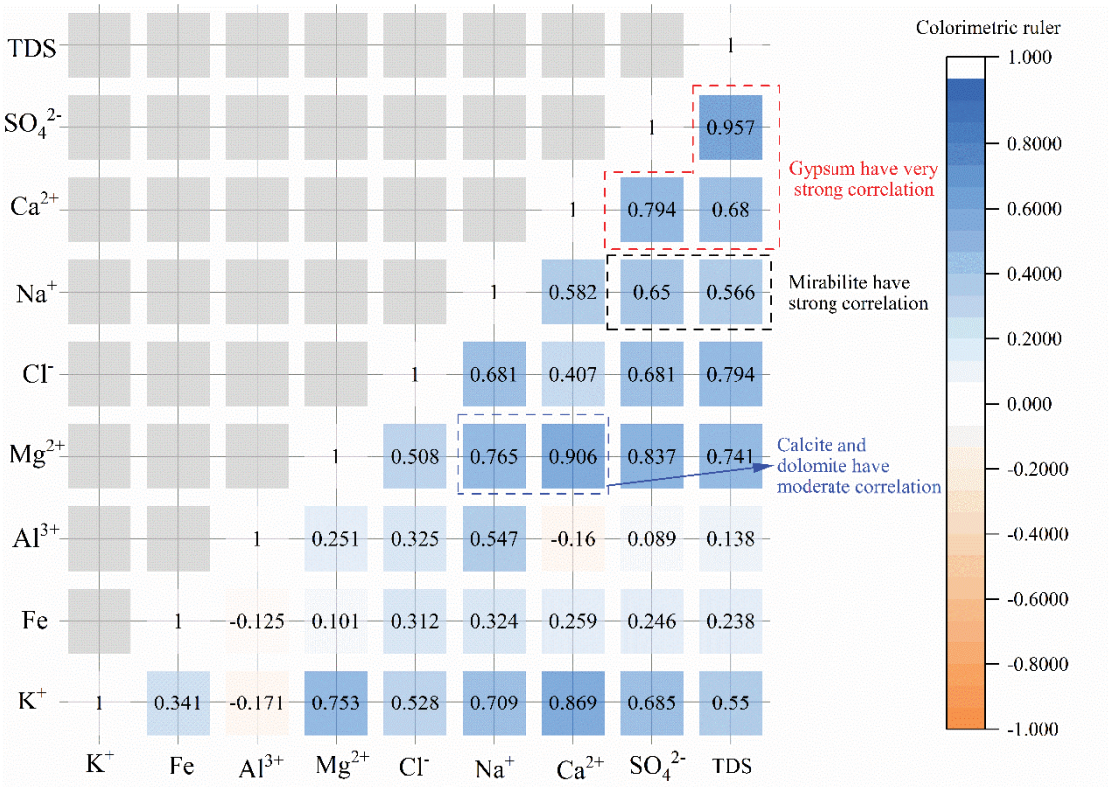

Fig. 6. Correlation coefficient diagram of water chemical parameters of the WGK4 water samples.

anions, cations, and TDS concentration in the water sample with time is displayed in Fig. 7.

Fig. 7a reveals that the TDS changes of the WGK4 water samples in the blank control group can be categorised into three stages: rapid increase during 0–2 d, slow decrease during 2–7 d, and slow increase during 7–35 d. In the first stage, sulfate minerals (e.g., mirabilite and gypsum) dissolved rapidly at the initial stage of soaking, the dissolution rate of rock minerals was higher than the sum of the adsorption rate and precipitation rate of clay minerals, the ion release amount was higher than the total amount of adsorbed and precipitated, and the ion concentration in the water body increased, and TDS increased [42]. In the second stage, the dissolution rate of sulfate minerals decreased, and clay minerals adsorption and $CaCO_3$ precipitation were the main reactions. The total amount of ions adsorbed and precipitated was greater than the number of ions released, and the TDS value abate due to ion concentration in water decreased. In the third stage, sulfate minerals dissolved continuously, and the precipitation rate of $CaCO_3$ and clay minerals decreased. At this time, the ion release amount was higher than the total amount of precipitation and adsorption, the ion concentration of the soaking solution increased, and TDS increased again.

3.4.2. Analysis of the TDS variation and key impact parameters of WGK1 water bodies

The data from the WGK1 immersion test are reported as the average of three parallel trials, with a maximum relative deviation of 1% (TDS) and 11% (general water chemical parameters). Fig. 8 shows the variation of main anions, cations, and TDS mass concentration in the water sample with time.

Fig. 8a reveals that the TDS change of the WGK1 water sample can be categorised into three stages: rise within 1 d, rapid decrease during 1–7 d, and slow decrease during 7–35 d. According to the WGK4 analysis of the blank control group, combined with the change in the main anions and cations in the WGK1 water sample and water body characteristics, the reasons for TDS changes are as follows: in the first stage, sulfate minerals dissolved rapidly at the initial stage of soaking, clay minerals absorbed and precipitated slowly, the ion release amount was higher than the total amount of ions absorbed and precipitated, the ion content in the soaking solution increased, and TDS increased [42]. In the second stage, the water pH is greater than 8, the adsorption rate such as clay minerals accelerated, and the initial concentration of calcium and magnesium ions in the water was higher. At this time, calcium and magnesium ions were mainly consumed, and the precipitation rate accelerated. The total number of ions adsorbed and precipitated was higher than the number of ions released, the ion content in the water decreased and TDS fell. In the third stage, sulfate minerals continued to dissolve, and the adsorption rate of clay minerals remained fast under the influence of pH, and the number of ions released was less than the total amount of ions adsorbed and precipitated. Therefore, the ion concentration in the water body, and the TDS value decrease.

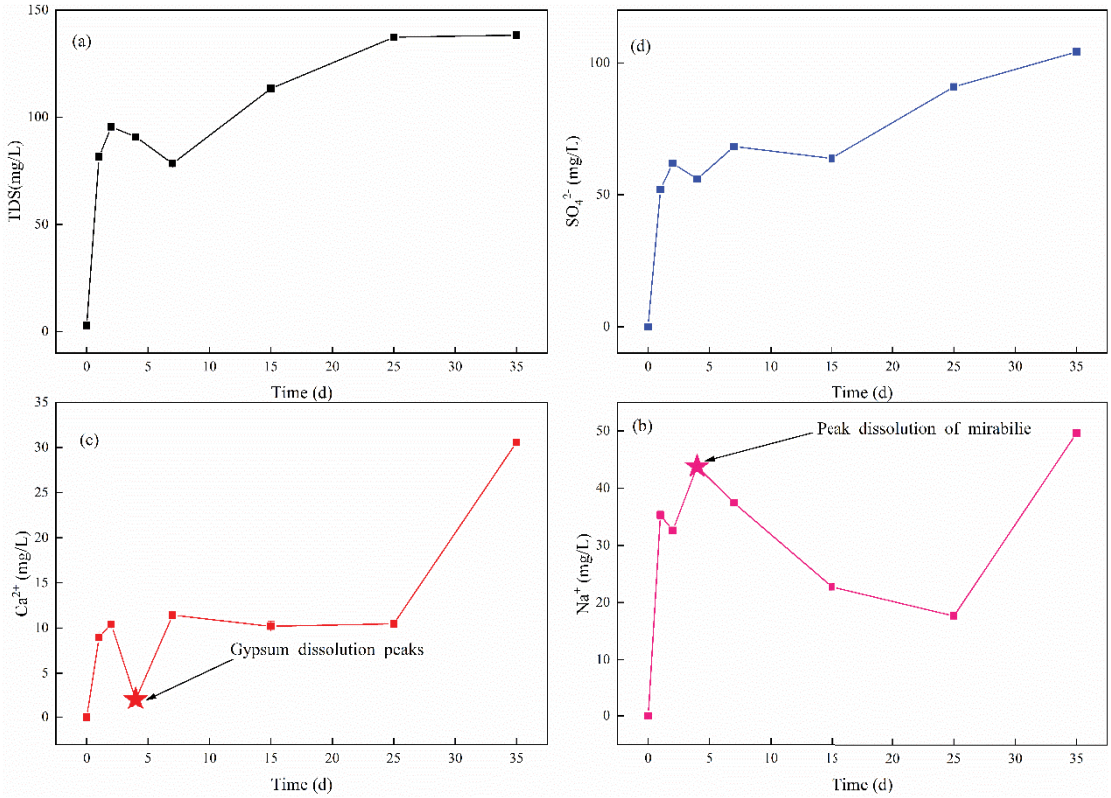

Fig. 7. Plot of main ions and total dissolved solids of the WGK4 immersion solution.

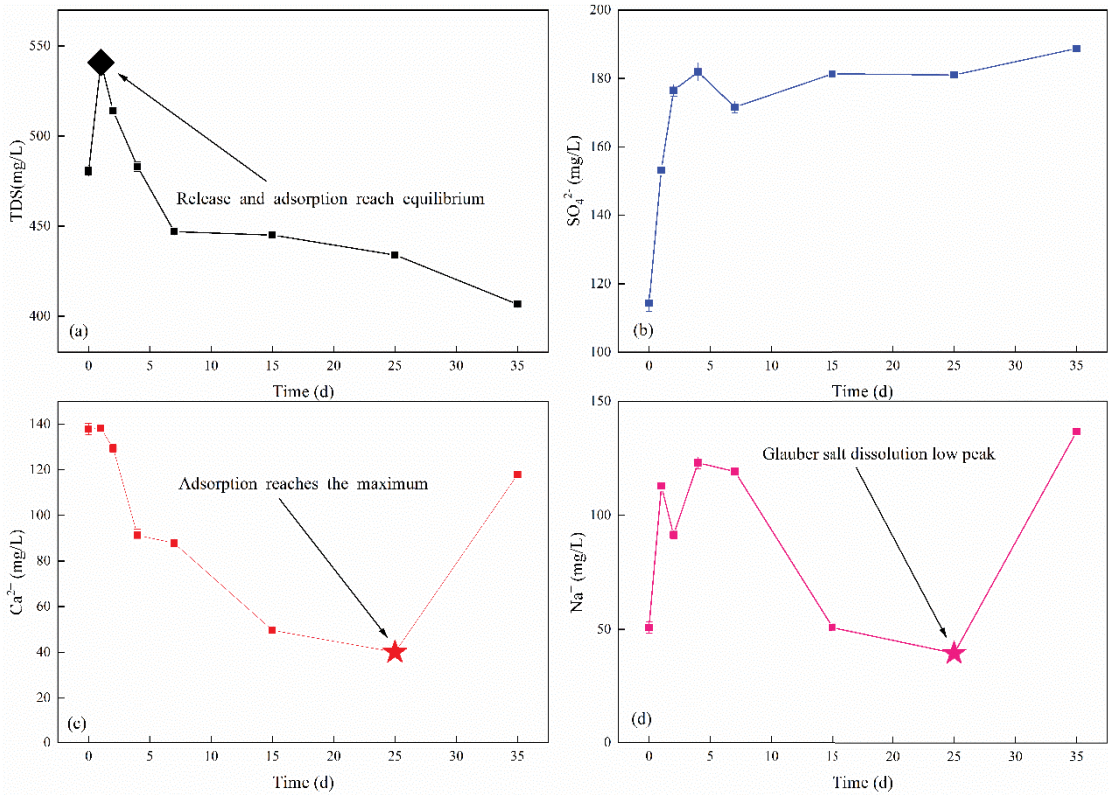

Fig. 8. Changes of main ions and total dissolved solids in WGK4 immersion solution.

3.4.3. Analysis of the TDS variation and key impact parameters of WGK2 water bodies

Data from the WGK2 immersion test are reported as the average of three parallel trials, with a maximum relative deviation of 1% (TDS) and 11% (general water chemical parameters). The variation law of the main anions, cations, and TDS concentration in the water sample with time is displayed in Fig. 9.

Fig. 9a reveals that the TDS change of the WGK2 water sample can be categorised into three stages: rapid increase within 1 d, decrease during 1–2 d, and slow increase during 2–35 d. According to the WGK4 analysis of the blank control group, combined with the change of the main anions and cations in the WGK2 water sample and water body characteristics, the causes of TDS change are as follows: in the first stage, sulfate minerals dissolved rapidly at the initial stage of soaking, the adsorption and precipitation rate of clay minerals were slow, the ion release number was higher than the total number of adsorbed and precipitated ions, the ion content of the soaking solution increased and TDS hoisted [42]. In the second stage, when the pH of the water exceeded 8, the adsorption rate of clay minerals and organic matter accelerated. At this time, the dissolution rate of minerals was less than the total rate of adsorption and precipitation, and the total number of ions adsorbed and precipitated was higher than the number of ions released. The ion concentration in water decreased and TDS declined. In the third stage, considerable sodium ions enriched in the water were adsorbed and ions exchange effect is strong, and the precipitation rate of $CaCO_3$ decreased. At this stage, the total amount of ions released was higher than the total amount of ions precipitated and adsorbed, the ion concentration increased in the soaking solution and TDS raised.

3.4.4. Analysis of the TDS variation and key impact parameters of WGK3 water bodies

The data from the WGK3 immersion test are reported as the average of three parallel trials with a maximum relative deviation of 1% (TDS) and 12% (general water chemical parameters). The variation law of the main anions, cations, and TDS concentration in the water sample with time is displayed in Fig. 10.

Fig. 10a reveals that the TDS change of the WGK3 water sample was categorised into three stages, which rapidly increased within 1 d, decreased during 1–4 d, and slowly increased during 4–35 d. According to the WGK4 analysis of the blank control group, combined with the change in the main anion and cation in the WGK3 water sample and water characteristics, the causes of TDS change are as follows: in the first stage, the initial pH and Na^+ concentration of the water body was higher, but the calcium and magnesium ion concentrations were lower, Na^+ ions were adsorbed by clay minerals and organic matter, and ion exchange is intense, rock minerals dissolved rapidly, precipitation rate was slow, the amount of ion released was higher than the total amount of adsorbed and precipitated ions, ion concentration in the water body increased, and the TDS value rise. In the second stage, the dissolution rate of rock minerals decreased, the

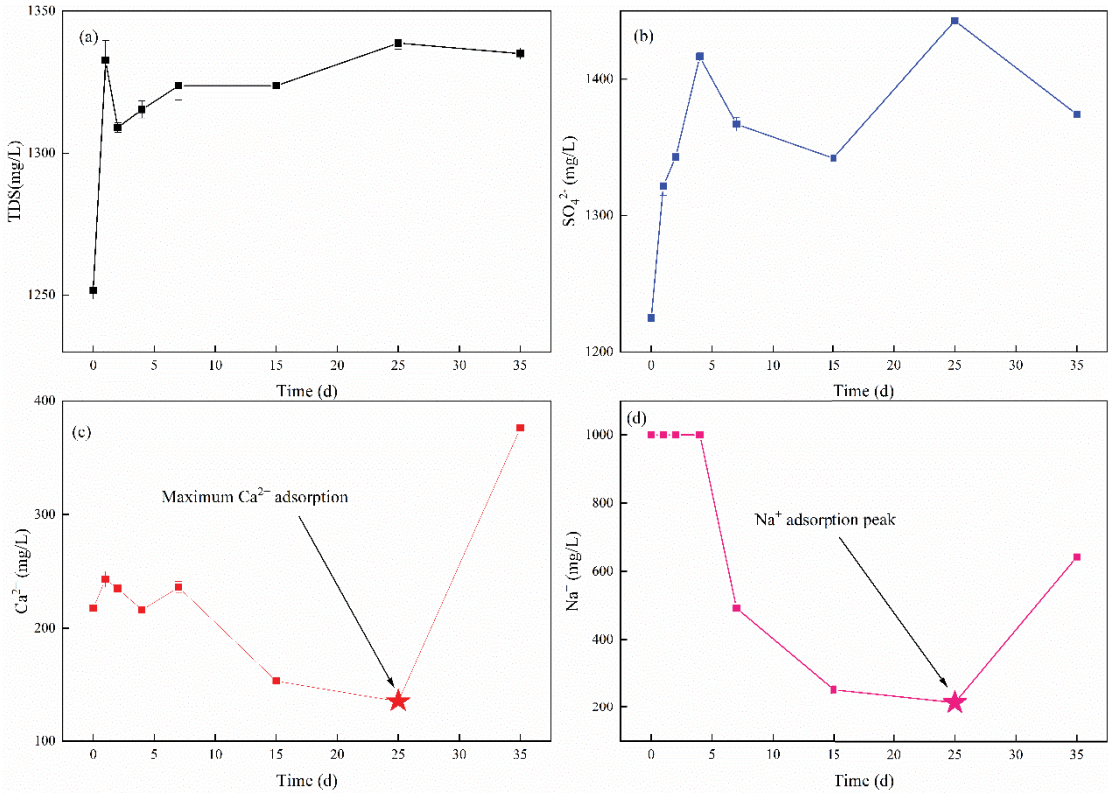

Fig. 9. Change of main ions and total dissolved solids of WGK2 immersion solution.

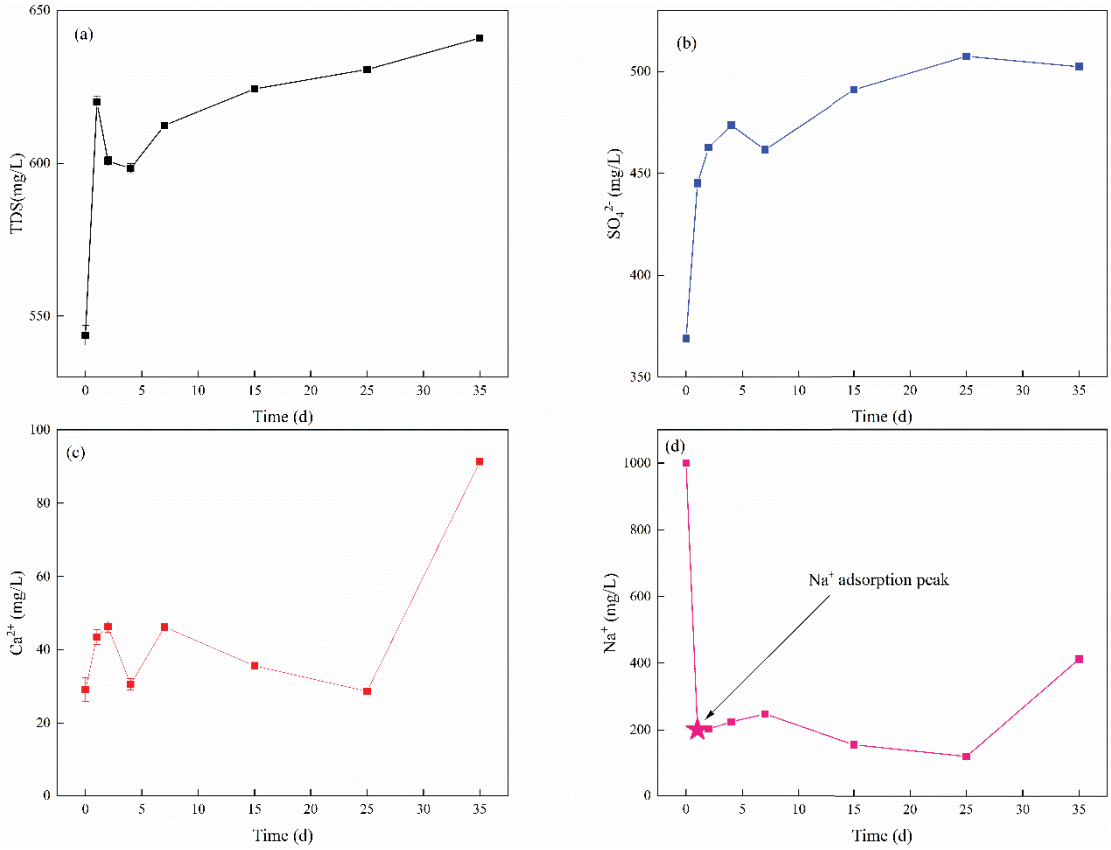

Fig. 10. Plot of main ion and total dissolved solids changes in WGK3 immersion solution.

adsorption and ion exchange of clay minerals continued, the total number of ions adsorbed and precipitated was higher than the number of ions released, and the ion concentration in water decreased and TDS fell. In the third stage, the precipitation rate of $CaCO_3$ decreased. With the continuous dissolution of rock minerals and the alternating adsorption of cations, the number of ions released was higher than the total number of adsorbed and precipitated ions, the ion concentration in water increased, and TDS hoisted.

The TDS change in the water-rock interaction system was influenced by many factors, such as the dissolution of rock minerals, authigenic precipitation, adsorption of clay minerals, and ion exchange. WGK4 was not affected by the initial pH and ion concentration of water, mainly by the dissolution rate of rock minerals and the adsorption as well as precipitation rates of clay minerals. Overall, it shows a changing trend of initial rise, followed by subsequent decline and then rise. The TDS change of the WGK1 water sample was mainly controlled by the adsorption rate of organic matter and clay minerals and the dissolution rate of rock minerals, and was affected by the initial pH and ion exchange. Overall, it shows a trend of initial rise, followed by a subsequent rapid decrease and then a slow decreasing. The TDS change of the WGK2 water sample was mainly controlled by the adsorption rate of organic matter and clay minerals and the dissolution rate of rock minerals. In addition, TDS was affected by pH change of the water body, initial cation concentration, and ion exchange. It shows a trend of initial rapid, followed by subsequent decline and slow rise. The TDS change of the WGK3 water sample was mainly controlled by the adsorption rate of organic matter and clay minerals, dissolution rate of rock minerals, and was affected by the initial cation concentration and ion adsorption. It shows a changing trend of initial rising, followed by subsequent decline and slow rise. For the karst water samples, the initial pH value, pH change, ion content, and ion exchange intensity affected the TDS change. All reactions are continued in the water-rock interaction system, the TDS change was mainly affected by the dissolution rate of rock minerals and the adsorption rate of clay minerals. When the total dissolved amount was higher than the total adsorbed amount, the TDS increased, and vice versa.

4. Conclusions

The XRD and XRF results of coal gangue are consistent. These results revealed that kaolinite and quartz are the main coal gangue, and that calcite, ankerite and sanidine are the secondary minerals. The quality of karst water in Baizhuang was excellent, but the ion levels in karst water in Zhai-zhen exceeded the standard, especially the levels of TDS and SO_4^{2-}.

The pH change of the soaking solution is affected by multiple factors, such as the acid/alkaline mineral concentration of coal gangue, cation exchange reaction, and pH value of karst water, however, the main controlling factor is the

mineral content of coal gangue. For karst water samples, the change in pH is influenced by the initial pH value and cation exchange cannot be ignored. The change in ORP of the soaking solution is related to the oxidation–acid production process of pyrite. The DO initial concentration, Fe^{3+} concentration, and pH value of karst water considerably affect the reaction. For karst water samples, Fe^{3+} ions in the initial water samples contribute considerably to the ORP change. The water-rock interaction reaction system between coal gangue and water is highly complex, TDS changes are affected by the comprehensive actions of rock mineral dissolution, secondary precipitation, clay mineral adsorption, ion exchange, and complexation reaction. However, calculating the contribution of each reaction to TDS changes is difficult, and the specific process should be analysed in future research. For the karst water samples, initial pH value, pH changes, higher initial concentration ion types, and ion concentration affect the process of TDS changes.

As a type of solid particle associated with coal, the composition of coal gangue is affected by complex factors, such as coal forming conditions, the environment, and temperature, and various coal gangues are formed in different regions and causes of environments. Therefore, determining the mineral composition and content of coal gangue in the study of the interaction system between coal gangue and the aqueous solution is critical for analysing the specific reaction and mechanism of material migration and transformation in coal gangue. Future studies on the mechanism of coal gangue for various types of karst water should focus on the influence of coal gangue minerals. Although the initial properties of karst water also affect the water quality change, the dissolution or adsorption of coal gangue minerals mainly plays a critical role in the water quality change.

Credit authorship contribution statement

Kaiming Ji was the main author of the manuscript and has made major contributions to the operation throughout the experiment, including data collection, data analysis and article conception. Dongjing Xu was responsible for leading the planning, execution, and the review of the research activities. He was also the main funder of the study. Jinjin Tian is mainly responsible for studying literature collection, analyzing the experiment data, and drawing the charts.Tiaohao Liu has contributed to the operation in experiment guidance, especially the guidance of the geological work and the data analysis.

Declaration of competing interest

The authors declare that they have no known competing financial interests or personal relationships that could have appeared to influence the work reported in this paper.

Acknowledgments

This work was supported by the National Natural Science Foundation Program (Grant 41572244), the National Natural Science Foundation of China (41807283), the Natural Science Foundation of Shandong Province (Grant ZR2015DM013), the National Natural Science Foundation of China (Grant 51804184), and the Scientific Research Foundation of Shandong University of Science and Technology for Recruited Talents (Grant 2017RCJJ031).

References

[1] K. Zhu, Notice of Retraction: Environmental Hazards and Comprehensive Utilization of Coal Gangue in Sustainable Development. 2011 5th International Conference on Bioinformatics and Biomedical Engineering, IEEE, Wuhan, China, 2011, pp. 1–4.
[2] C.M. Ma, L.H. Zhao, 178 Environmental Problems of Coal Gangue Air Storage in Pingdingshan Mining Area and Prevention and Remediation Countermeasures, ASME Press Select Proceedings, Geological Engineering: Proceedings of the 1st International Conference (ICGE 2007), ASME Press, 2009, doi: 10.1115/1.802922.paper178.
[3] D. Ma, H.Y. Duan, J.F. Liu, X.B. Li, Z.L. Zhou, The role of gangue on the mitigation of mining-induced hazards and environmental pollution: an experimental investigation, Sci. Total Environ., 664 (2019) 436–448.
[4] M.T. Gao, M. Zhang, M. Zhou, Study and practice on the technology of filling mining in Xin Wen mining area, Appl. Mech. Mater., 121–126 (2011) 2892–2896.
[5] W.B. Zhang, H.B. Song, Comprehensive utilization of the solid wastes from coal in China, J. Kunming Univ. Sci. Technol., 4 (2000) 15–18,24.
[6] L.F. Yang, Practice and research of comprehensive utilization of coal gangue in Xiqu Mine, Shandong Coal Sci. Technol., 7 (2020) 200–201,210.
[7] Y.F. Luo, Y.G. Wu, T.L. Fu, H. Wang, R.R. Xing, Z.L. Zheng, Effects of a proline solution cover on the geochemical and mineralogical characteristics of high-sulfur coal gangue, Acta Geochim., 37 (2018) 701–714.
[8] T. Yang, X.Y. Chen, X. Liu, L.G. Zheng, Environmental geochemical characteristics of cadmium of soil and coal gangue in mining-induced subsidence area of Panji mine in Huainan, Coal Geol. Explor., 46 (2018) 1–5.
[9] J.S. Fan, Y.Z. Sun, X.Y. Li, C.L. Zhao, D.X. Tian, L.Y. Shao, J.X. Wang, 2013. Pollution of organic compounds and heavy metals in a coal gangue dump of the Gequan Coal Mine, China, Chin. J. Geochem., 32 (2013) 241–247.
[10] Y. Wang, Y.J. Zou, H. Wang, C.B. Wang, Geochemical characteristics of Se and heavy metal elements in the soil of Youshan, Xinfeng County, Jiangxi Province, N.a. N.a. Geol., 2 (2019) 152–160.
[11] W. Pian, J.K. Zhang, J.X. Wang, et al., Environmental pollution of surrounding groundwater from coal gangue leaching in mining area, J. Hebei Univ. Eng. (Nat. Sci. Ed.), 33 (2016) 80–84,108.
[12] W.Y. Qi, Y.L. Huang, H. He, J.X. Zhang, J.M. Li, M. Qiao, Potential pollution of groundwater by dissolution and release of contaminants due to using gangue for backfilling, Mine Water Environ., 38 (2019) 281–293.
[13] C.Y. Hua, G.Z. Zhou, X. Yin, C.Z. Wang, B.R. Chi, Y.Y. Cao, Y. Wang, Y. Zheng, Assessment of heavy metal in coal gangue: distribution, leaching characteristic and potential ecological risk, Environ. Sci. Pollut. Res., 25 (2018) 32321–32331.
[14] M. Chen, L.J. Zhu, Y.G. Wu, T.L. Fu, Y. Ran, Enrichment of heavy metals in coal gangue by puff balls and mechanism research, Chin. J. Geochem., 4 (2014) 419–424.
[15] J. Yang, J.J. Chen, X.Y. Wang, X.H. Li, Heavy metal concentrations distribution around the coal gangue pile of Yanma Mine, Res. Environ. Sci., 1 (2008) 90–96.
[16] C. Zhou, G. Liu, Z. Yan, T. Fang, R. Wang, Transformation behavior of mineral composition and trace elements during coal gangue combustion, Fuel, 97 (2012) 644–650.
[17] C. Zhu, S.J. Qu, J. Zhang, Y. Wang, Y.H. Zhang, Distribution, occurrence and leaching dynamic behavior of sodium in Zhundong coal, Fuel, 190 (2017) 189–197.
[18] X.C. Wang, Hydrogeological condition analysis of 3 coal seam in Hong-qi coal mine, Jia-xiang, Shandong Coal Sci. Technol., 5 (2017) 117–119.

[19] Y.P. Wang, Research on Water Inrush Prevention Technology of Coal Seam Floor Lagging in Baizhuang Mine, N.a. Univ. Min. Technol., 2019.
[20] H.Y. Yin, J.C. Wei, Y. Wang, J.B. Guo, L.Q. Shi, Risk evaluation of water inrush from seam floor during mining of lower group in Zhaizhen coal mine, N.a. Min. Mag., 18 (2009) 97–99.
[21] L.Q. Shi, R.A. Zhang, D.J. Xu, et al., Prediction of water inrush from floor based on GWO-Elman neural network, J. China Coal Soc., 45 (2020) 2455–2463.
[22] J.S. Zhang, et al., Minerals in the No. 3 Coal Seam and its Surrounding Rock in Juye Coalfield, Proceedings of the 9th National Congress and the 16th Annual Conference of the Chinese Society of Mineralogy, Petrology and Geochemistry, 2017, p. 1220.
[23] S.F. Dai, Y.F. Jiang, C.R. Ward, L.D. Gu, V.V. Seredin, H.D. Liu, D. Zhou, X.B. Wang, Y.Z. Sun, J.H. Zou, D.Y. Ren, Mineralogical and geochemical compositions of the coal in the Guanbanwusu Mine, Inner Mongolia, China: further evidence for the existence of an Al (Ga and REE) ore deposit in the Jungar Coalfield, Int. J. Coal Geol., 98 (2012) 10–40.
[24] State Bureau of Technical Supervision, Quality Standard for Ground Water, GB/T 14848-93, 1993.
[25] L.G. Jiang, B. Liang, C.W. Yin, Experimental study of coal gangue acid/alkali production kinetics in the leaching effect, J. Exp. Mech., 4 (2013) 502–510.
[26] B. Li, Geochemistry Effect of Gangue Leaching and Its Potential Risk—Take the Hancheng Coal Area as an Example, Chang'an Univ., 2013.
[27] Z. Ran, W.L. Liu, Y.T. Pan, W. Liu, Z. Gao, Y. Zhao, Influence of temperature on dynamic leaching characteristics of coal gangue, J. N.a. Coal Soc., 44 (2019) 1239–1246.
[28] Q.F. Liu, L.T. Liu, S.L. Ding, The water-solubility and exchangeability of NH_4^+ in ammonium illite, Acta Miner. Sin., 30 (2010) 278–282.
[29] X. Zhang, X.J. Li, Leaching Experiment and Leaching Characteristics of Heavy Metals From Coal Gangue in Jining Mining Area, The 8th National Conf. on Land Reclam. and Ecol. Restor. in Min. Areas of N.a. Coal Soc., Jiaozuo, Henan, China, 2019, pp. 311–323.
[30] Z. Dang, C.Q. Liu, Z. Li, Experimental simulation of chemical activity of heavy metals in coal gangue, J. N.a. N.a. Univ. Technol. (Nat. Sci.), 29 (2001) 1–5.
[31] Y.Q. Zhang, M.H. Hung, F.F. Qi, Y. Du, The leaching characteristics of metals and acid radical ions in gangue, Environ. Chem., 3 (2014) 452–458.
[32] W.H. Ao, Study on the Geochemical Effects of Harmful Substances in Coal Gangue in Wuda Mining Area, Inner Mongolia, N.a. Univ. Geosci. (Beijing), 2005.
[33] Y. Zhao, L.P. Wang, S.L. He, M. Hou, X. Chen, L. Zhang, Variation of ORP during *p*-nitrophenol degradation by Fenton oxidation process, Environ. Pollut. Control, 4 (2011) 58–61,65.
[34] W.R. Jiang, Z.H. Tu, S. Zhou, Q. Wu, Z. Dang, H.J. He, et al., A brief overview on the mechanism and kinetic influencing factors of the pyrite surface oxidation, Met. Min., 50 (2021) 88–102.
[35] Z.H. Tu, Studies of Sulfur Transformation in Oxidation of Pyrite and Surface Electrochemistry of Pyrite Oxidation, N.a. N.a. Univ. Technol., 2017.
[36] G.K. Druschel, R.J. Hamers, J.F. Banfield, Kinetics and mechanism of polythionate oxidation to sulfate at low pH by O_2 and Fe^{3+}, Geochim. Cosmochim. Acta, 67 (2003) 4457–4469.
[37] C.O. Moses, D.K. Nordstrom, J.S. Herman, A.L. Mills, Aqueous pyrite oxidation by dissolved oxygen and by ferric iron. Geochim. et Cosmochim., 51 (1987) 1561–1571.
[38] L. Lu, R.C. Wang, J.Y. Xue, et al., Experimental study on oxidation rate of pyrite, Sci. N.a. Rress (Series D), 35 (2005) 434–440.
[39] Z.J. Zhang, Y.N. Li, Z.Y. Tong, H. Nong, X. Chen, Adsorption characteristics of metal ions on kaolinite, J. Min. Sci. Technol., 3 (2017) 294–300.
[40] H.-H. Wu, P.-H. Liu, Q.-Y. Zhang, G.-P. He, Mechanisms of adsorption of heavy metal ions on kaolinite and their solution as a function of pH, Geol. J. N.a. Univ., 1 (2005) 85–91.
[41] Z.Y. Fang, Research on Mechanism of Purifying Underground Reservoir Water Storage by Collapsed Coal Rock in Goaf of Wanli No. 1 Coal Mine, N.a. Univ. Min. Technol., 2020.
[42] K. Zhang, J. Gao, B.B. Jiang, J. Han, M. Chen, Experimental study on the mechanism of water-rock interaction in the coal mine underground reservoir, J. N.a. Coal Soc., 12 (2019) 3760–3772.